6. CHARACTER OF THE DÉCOLLEMENT IN THE LEG 131 AREA, NANKAI TROUGH[1]

G.F. Moore[2] and T.H. Shipley[3]

ABSTRACT

The décollement under the Nankai Trough accretionary prism in the Leg 131 area is imaged seismically as a high-amplitude, reversed-polarity reflection. The décollement is a 19-m-thick zone of intense brecciation where it was penetrated on Leg 131. Physical properties measurements at Site 808 indicate that the strata beneath the décollement have lower velocities and densities than overlying strata. The seismic signature of the décollement varies considerably along both strike and dip. The lateral amplitude variations could be due to: (1) tuning effects as the layer thickens and thins, (2) focusing and defocusing of seismic energy due to the complex overlying structure, or (3) velocity variations caused by changes in porosity as fluid pressures dilate zones within or beneath the décollement. Synthetic seismic models show that the décollement signature can best be modeled by a sharp decrease in velocity and density beneath the décollement. Numerous models with a range of reasonable overlying structures were explored to examine the lateral amplitude variations. Based on these models, the variations in amplitude cannot be completely explained by focusing/defocusing of rays by the complex overlying structure or by changes in velocity/density of the underlying strata. The thickness of the décollement zone is very close to its tuning thickness, so tuning effects can explain much of the amplitude variations. The changes in amplitude are therefore caused by lateral changes in velocity, density, and thickness of the décollement, which are in turn probably driven by fluid pressure variations within the décollement zone.

INTRODUCTION

One of the major targets of drilling on ODP Leg 131 was the décollement at the base of the accretionary prism. Seismic profiles show a prominent reflection along the basal décollement that extends seaward under the trench wedge and landward beneath the accretionary prism (Moore et al., 1990, 1991). Leg 131 drilling at Site 808 penetrated the décollement and sampled the strata above and below it (Figs. 1, 2). The décollement zone itself was a region of poor recovery, however, so the nature of the zone remains poorly understood. Physical properties measurements do not constrain the velocity of the décollement, so it could be a zone of either high or low velocity. The two have fundamentally different implications for fluid flow within and below the décollement.

Drilling into the Barbados accretionary prism showed the décollement to be a zone of fluid transport (Moore et al., 1988). Bangs and Westbrook (1991) modeled this décollement reflection as a thin zone of low velocity and density. They attributed lateral changes in amplitude of the décollement reflection to lateral changes in velocity of the décollement zone.

This paper investigates the character of the décollement in the Leg 131 area of the Nankai Trough. We combine the results of regional seismic interpretations of the décollement with synthetic seismic modeling, based on physical property measurements made at Site 808.

DATA ACQUISITION AND PROCESSING

The seismic data used in this study were collected on the *Fred Moore* in July 1987 (Fig. 1) with a 1065 in3 (17.5 L) array made up of six air guns of various chamber sizes. The seismic signals were received with a 68-channel hydrophone array with 33.3-m group spacing, sampled at 2 ms and recorded in demultiplexed format (SEG-D) on magnetic tape. Processing consisted of common midpoint (CMP) sort, resample to 4 ms, velocity analysis, normal moveout (NMO) correction, stack, deconvolution, filter, finite-difference time migration, and depth migration. Details of the acquisition and original processing are described in Moore et al. (1990 and 1991). Prior to the seismic modeling described below, reprocessing was undertaken to preserve as much of the original source waveform and reflection amplitude information as possible. This was accomplished by starting with the CMP-sorted data at 2-ms sample interval, careful editing of bad shots and traces, NMO correction, and stacking of only the near 12 traces of each CMP (170–703 m) to eliminate effects of CMP stretch and amplitude variations with offset. Deconvolution was eliminated to prevent wavelet modifications. A relatively broad-band, time-varying filter (10-15-40-50 Hz at the level of the décollement) and spherical divergence (t2) gain were applied after stack (Fig. 3). Although the depth-migrated section was used to construct the seismic depth models, only the stacked section was used for comparison to the detailed models because of the possibility of amplitude and waveform distortion in the migration process.

CHARACTER OF THE DÉCOLLEMENT

Structural and Physical Properties Expression

The décollement was penetrated at Site 808 and is defined structurally as a 19.2-m-thick zone of intense faulting and brecciation beginning at 945 m in Hole 808C (Shipboard Scientific Party, 1991). There is a marked structural contrast between the relatively undeformed underthrusting strata beneath the décollement and the more strongly deformed prism material above the décollement (Shipboard Scientific Party, 1991).

The décollement is also easily identified in physical properties measurements (Shipboard Scientific Party, 1991). Velocities in samples above the décollement increase approximately linearly from about 1750 m/s at 400 mbsf to more than 2250 m/s just above the décollement. Velocities drop sharply to less than 2100 m/s just below the décollement. Bulk densities show a parallel increase to the top of the décollement and decrease below the décollement. Samples within the décollement zone have very high velocities (2300–2400 m/s) and high densities (2.26–2.35 g/cm^3). It is not clear, however, whether these velocities and densities reflect the bulk physical properties of the décollement zone or whether they are valid only for isolated coherent blocks.

[1] Hill, I.A., Taira, A., Firth, J.V., et al., 1993. *Proc. ODP, Sci. Results*, 131: College Station, TX (Ocean Drilling Program).
[2] Department of Geology and Geophysics, University of Hawaii, Honolulu, HI 96822.
[3] University of Texas Institute for Geophysics, Austin, TX 78759-8345.

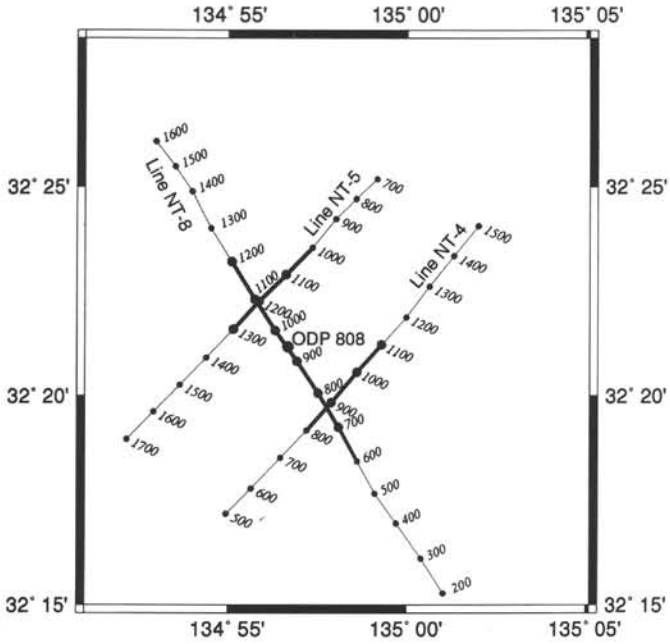

Figure 1. Location of seismic lines across the Nankai trough used in this study. Bold portions of lines are those segments illustrated in later figures. Annotations are CMP numbers.

Seismic Expression

The décollement is imaged seismically at Site 808 as a reflection at 7.15 s (Fig. 3) with a polarity reversed from the water bottom reflection (Fig. 4). The décollement reflection is a reversed-polarity reflection seaward under the trench wedge and continues landward under the accretionary prism to at least 30 km from the frontal thrust (Fig. 2; Moore et al., 1990). Strike lines also show that the décollement reflection extends laterally throughout the survey area (Fig. 5) with considerable variation in character and amplitude. This variation is most noticeable on the strike lines. The character of the décollement is thus variable in three dimensions.

Seismic Modeling

Physical properties measurements demonstrate that the strata below the décollement are reduced in both velocity and density with respect to the overthrusting accretionary complex. It is of interest to know whether this velocity/density reduction is sufficient to produce the observed décollement reflection or whether the acoustic signature is influenced by a high or low impedance décollement zone.

To determine the nature of the décollement zone, we conducted waveform modeling using the 2D-AIMS modeling package from GeoQuest Technology. Velocities for the models were defined from physical properties measurements at Site 808 and extrapolated laterally using seismic reflection stacking velocities (Moore et al., 1990) and two-ship split-spread velocity profiles (Stoffa et al., 1992). AIMS calculates density (ρ) from Gardner's equation (Gardner et al., 1974): $\rho = 0.23\ V^{0.25}$. This is a reasonable approximation to the velocity-density relationship at Site 808. Preliminary models were generated by a relatively fast ray-trace algorithm, but final models utilized full wave-equation methods.

Wavelet Estimation

To carry out seismic modeling, a reasonable estimate of the source wavelet was required. We stacked water bottom reflections from several CMPs along the seismic line. Areas with dipping sub-bottom reflections were chosen so that the sub-bottom reflections would cancel, leaving only the water bottom reflection. Because the zone of interest for modeling is less than 20 m thick, and therefore less than one-half wavelength of our seismic data (see discussion below), we did not include any bubble-pulse effects in our estimated wavelet. The estimated wavelet is shown as the water-bottom reflection in Figure 6, consisting of a low-amplitude negative (unshaded) lobe followed by nearly equal-amplitude positive (shaded) and negative lobes. Theoretical models of the wavelet produced independently with modeling software from Seismic Research and Development Corporation are very similar to our derived wavelet.

To estimate the effects of wavelet broadening due to loss of high frequencies with depth, we calculated the frequency response from different sub-bottom depths. The amplitude spectra from water bottom (6.0 s) to 1 s sub-bottom is not significantly different from the spectra at 6.5 to 7.5 s (across the décollement) or from 7.0 to 8.0 s (below the décollement). Thus, we are confident that we can use our estimated wavelet for the synthetic models without fear that the waveform changes significantly with depth.

One-Dimensional Models

Our first concern in producing seismic models is whether or not our data can resolve the 19-m-thick décollement zone. Most authors agree that high-quality, low-noise seismic data can resolve the top and

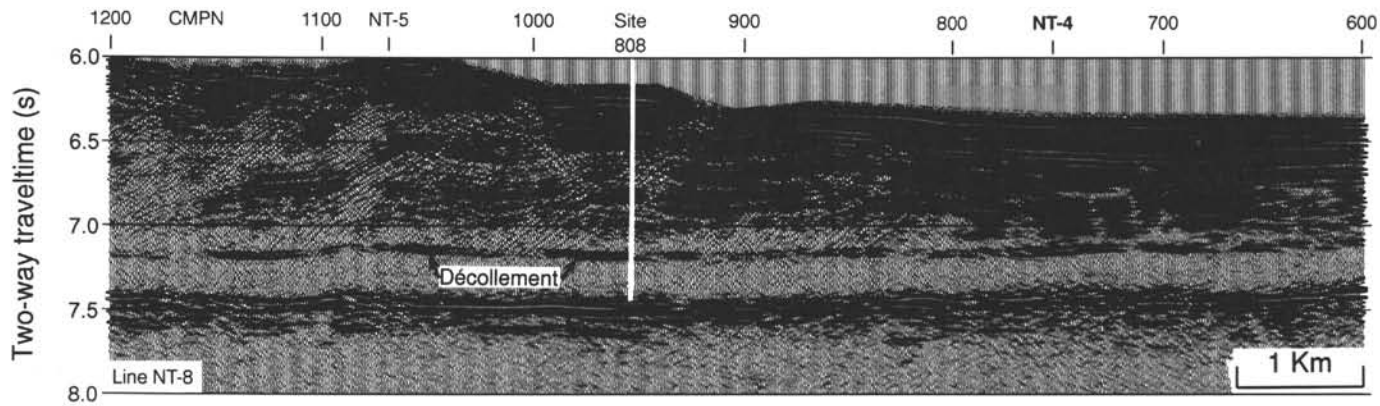

Figure 2. Portion of time-migrated seismic Line NT-8 through the Leg 131 area (after Moore et al., 1990), showing lateral variations in décollement amplitude. Section is plotted without automatic gain control to show true relative amplitudes. Locations of cross lines NT-4 and NT-5 (Fig.4) are indicated at top of section. See Figure 1 for location of line.

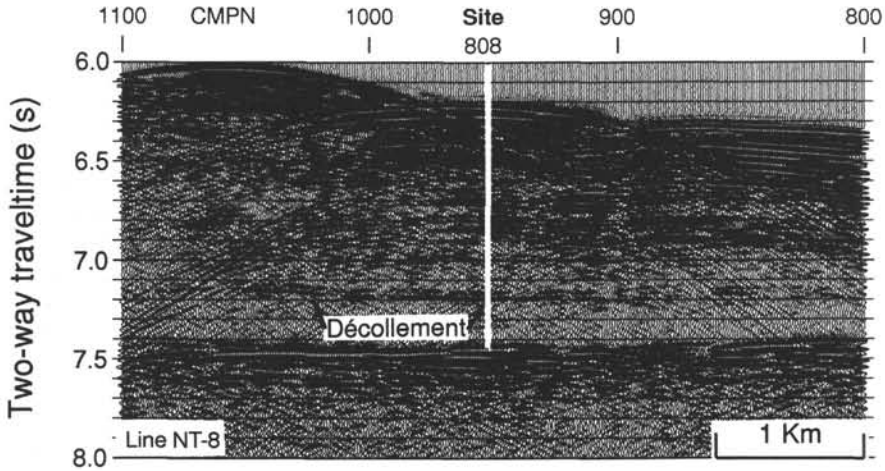

Figure 3. Reprocessed (stacked, but unmigrated) time section of Line NT-8. Note lateral variations in amplitude of décollement reflection.

bottom of a bed that is at least one-quarter wavelength thick (see for example, Kallweit and Wood, 1982; Sheriff, 1985). For a bed with a seismic velocity of V and a wavelet with a dominant frequency f, the quarter wavelength is simply $V/4f$ (Sheriff, 1985). In the case of the Nankai décollement, the velocity is about 2200 m/s (see above); the maximum frequency content of our seismic data at the depth of the décollement is greater than 40 Hz. Thus, a quarter wavelength is less than 2200/4×40 = 13.75 m. Our seismic data should therefore be able to resolve both the top and bottom of the 19-m-thick décollement zone if it has sufficient impedance contrasts at both interfaces.

We considered five possible impedance contrasts at the décollement (Fig. 6): (1) a negative contrast at the top of the décollement with a positive contrast at the base (model trace 1); (2) a negative contrast at the top of the décollement with another negative contrast at the base (model trace 2); (3) a décollement zone with the same velocity as the overlying strata and a negative contrast at the base (model trace 3); (4) a single negative contrast at the base (or top) of the décollement, which implies that there is no expression of the décollement (model trace 4); and (5) a positive impedance contrast at top of the décollement zone, with negative contrast below (representing the physical properties measurements that were made on recovered samples).

The seismic waveform of the décollement zone is a low-amplitude positive lobe followed by a stronger negative lobe followed by a similar amplitude positive lobe (Fig. 4). The synthetic waveforms of the décollement zone show that the worst match is for a zone with negative impedance contrasts at both the top and base of the décollement (Fig. 6, model trace 2). A positive contrast at the top and a negative contrast at the base yields a waveform (Fig. 6, model trace 5) that is of the correct shape, but the upper positive lobe is of higher amplitude than the lower lobe, so we consider this a poor match. Model traces 3 and 4 are nearly indistinguishable; both closely match the seismic data. Model trace 1 also exhibits the correct shape, but the leading positive pulse is somewhat low in amplitude. Several data

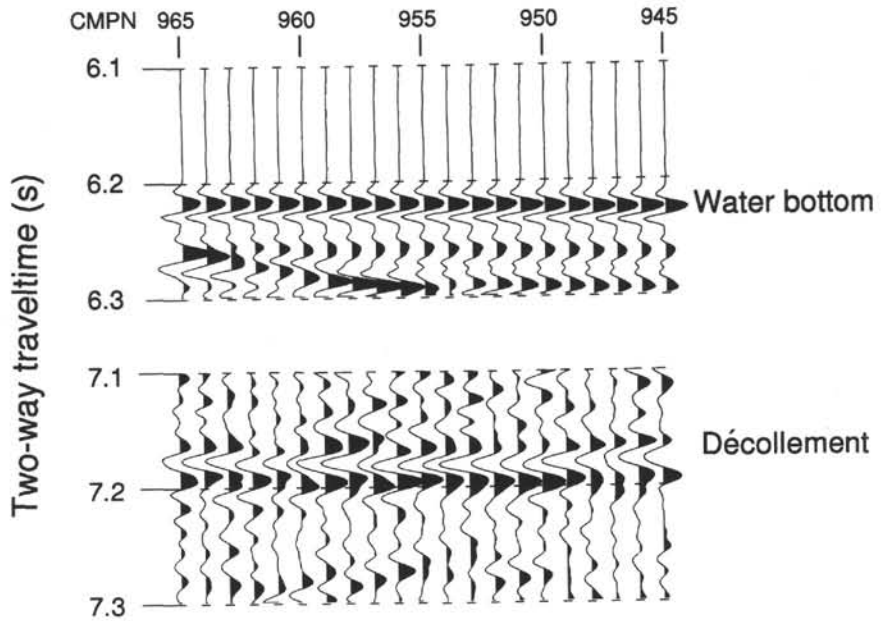

Figure 4. Detail of reprocessed stacked time section showing positive water bottom reflection and reversed-polarity décollement reflection. Positive amplitude side of waveform is shown in black.

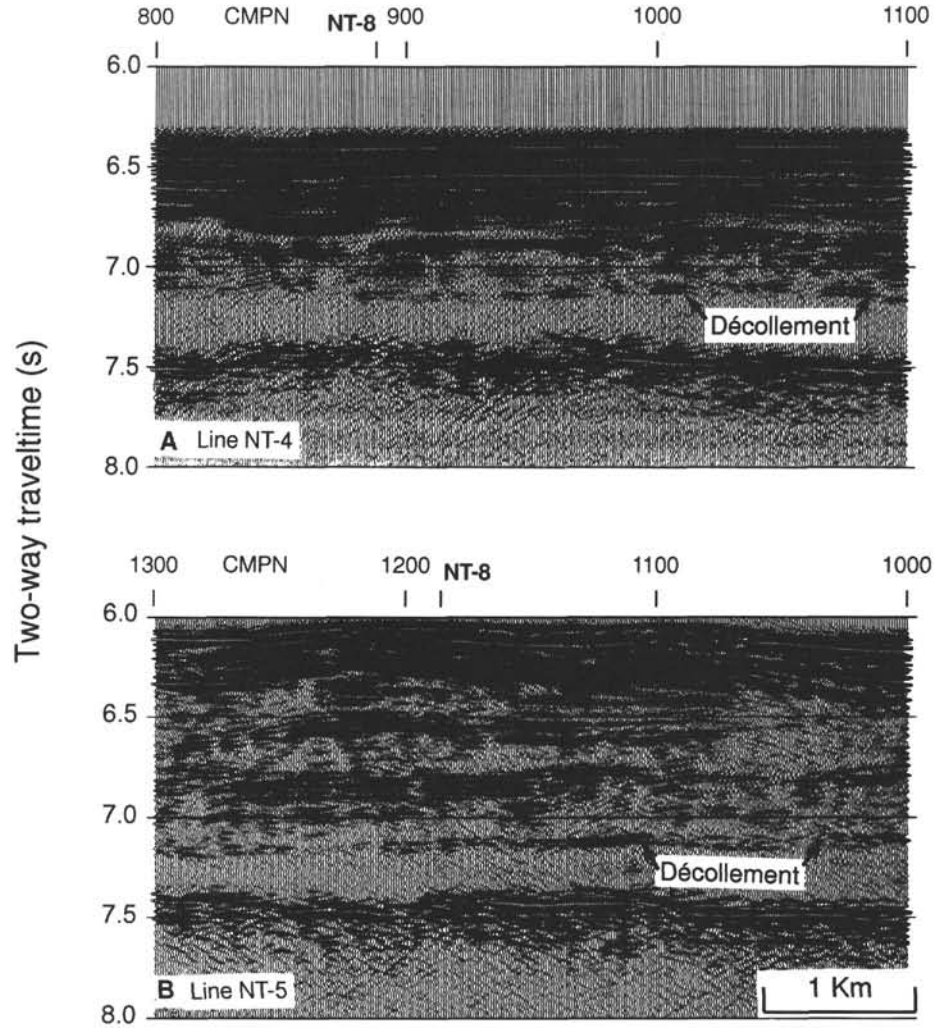

Figure 5. Time-migrated sections parallel to trench. Locations of crossings with Line NT-8 (Fig. 2) are indicated. See Figure 1 for location of lines. **A.** Line NT-4. **B.** Line NT-5.

traces, however, are similar to Model trace 1 (e.g., Figure 4, CMP# 961 and 962). Our models, therefore, indicate that much of the décollement waveform can be modeled by a single negative impedance contrast at the base (or top) of the décollement zone. A 20-m-thick décollement zone cannot have a significantly higher impedance than the overlying strata and match the observed waveforms (i.e., model 5); nor can it have an impedance intermediate between the overlying and underlying strata (i.e., model 2). It is also possible that the décollement, in some areas, might be a zone of significantly lower impedance than the underlying strata (i.e., model 1).

Two-Dimensional Modeling

We also constructed a series of two-dimensional synthetic seismic models to investigate the lateral changes in amplitude of the décollement reflection. These models included the complex prism structure (Fig. 7C) so that the effect of focusing/defocusing by the overlying structure could be evaluated.

Rays incident on a dipping interface that has a velocity contrast across it are refracted in a predictable manner according to Snell's law. This effect distorts ray paths and may affect the amplitudes of reflections from underlying interfaces. For instance, a wedge of high-velocity strata thrust over lower velocity strata can act as a distorting lens and disrupt the reflection from a continuous interface beneath (Badley, 1985). The effect is illustrated in diagrams showing ray paths from a single shot (Fig. 7A) and from a series of stacked (zero offset) records (Fig. 7B). Both ray-trace diagrams show that ray bending leads to areas on the décollement surface where ray bounces are concentrated (focused) or more widely spaced (defocused). This could lead to increases in amplitude of the décollement reflection where rays are focused and decreases in amplitude where rays are defocused. The resulting synthetic seismogram for this complex structure shows that, although amplitudes are affected by focusing and defocusing (Fig. 8), the magnitude is much smaller than the variations observed in the field seismic data (Fig. 3). Other explanations must therefore be sought for the changes in amplitude of the décollement reflection.

To further investigate the abrupt changes in décollement reflection amplitude, we ran a series of two-dimensional models in which the impedance of the layer beneath the décollement zone varied. Decreasing the impedance beneath the décollement decreases the amplitude of the negative reflection, but the waveform does not change shape as in our seismic data (Figs. 3, 5).

Tuning Effects

It is well known that the interference of reflections from the top and base of such a thin bed causes changes in the overall wave shape.

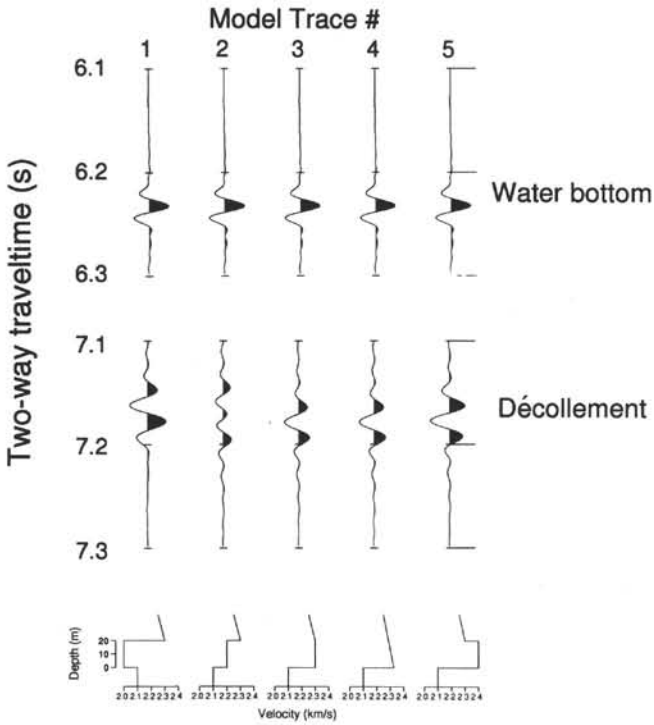

Figure 6. Water bottom-derived source wavelet, synthetic seismic model traces of water bottom and décollement, and velocity model for synthetic seismogram. Compare to Figure 4.

These changes yield information on the thickness of the bed (Widess, 1973; Neidell and Poggiagliolmi, 1977; Meckel and Nath, 1977; Knapp, 1990). When the layer thickness is less than about one-fourth of the seismic wavelength, distinct reflections from the top and base of the layer cannot be resolved. Instead, information on the thickness of the bed can be estimated by examining the composite waveform from the two interfering events (Widess, 1973). This is referred to as the "tuning effect." One-quarter wavelength for our seismic data is about 14 m (see above), which is very close to the thickness of the décollement zone drilled at Site 808. It is therefore possible that tuning might be affecting the amplitudes of the décollement reflection if the zone varies in thickness.

To investigate the possibility of tuning, we examined a series of wedge models (Fig. 9). In these models, the décollement was modeled as a wedge that thinned from 101 m to 1 m in thickness (Fig. 9A). Each wedge model has an upper layer of velocity 2300 m/s, corresponding to the Shikoku Basin strata overlying the décollement and has a velocity of 2100 m/s at the base of the décollement zone. Three models are illustrated in Figure 9, one with a low-velocity décollement zone (Fig. 9B), one with an intermediate-velocity zone (Fig. 9C), and one with a high-velocity zone (Fig. 9D). Although the seismic response of each wedge is different in detail, each shows the change in amplitude as the décollement zone thins below one-quarter wavelength. It is apparent that either a low-velocity décollement zone or an intermediate velocity zone can produce a waveform similar to our seismic data. As the low-velocity wedge thins below about 22 m, the lower lobe of the waveform sharpens and increases in amplitude. The intermediate velocity wedge produces waveforms of the correct shape at thicknesses below about 12 m. As a high-velocity zone decreases in thickness, the upper lobe of the waveform broadens and the lower lobe decreases in amplitude. Thus, a high-velocity wedge thinner than 20 m does not match the seismic data.

The wedge models provide insights into how changes in thickness and velocity of the décollement zone affect the waveform of the décollement reflection. We were then able to generate models in which both the thickness and velocity of the décollement zone varied in two dimensions (Fig. 10). We were able to closely match the waveform changes by varying the thickness of the décollement zone between 19 and 12 m, combined with impedance contrasts generated by changing the velocity between 2000 and 2200 m/s. The overlying and underlying velocities were held constant.

DISCUSSION

The negative polarity seismic reflection at the level of the décollement in the Leg 131 area extends from beneath the seaward margin of the trench wedge landward for several tens of km beneath the accretionary wedge. Our seismic models suggest that the Nankai décollement is a zone of variable thickness and acoustic impedance (velocity × density). The main physical requirement is that the negative reflection is caused by the reversal in impedance at the base of the décollement observed at Site 808. Our waveform modeling shows that the high velocities and densities measured on core samples from the décollement zone are valid only for those isolated samples and are not representative of the velocity and density of the zone as a whole. The décollement therefore is probably a zone of similar or lower velocity and density compared to the overlying strata.

The décollement reflection varies laterally in both amplitude and waveform. Our models show that, although lateral variations in amplitude can be explained by variations in the velocity/density of the strata beneath the décollement, lateral variations in waveform cannot be explained in this way.

Variations in the waveform and amplitude of the décollement reflection are best explained by lateral changes in the thickness, velocity, and density of the décollement zone. This interpretation is consistent with ideas presented by Bangs and Westbrook (1991) for the Barbados décollement and by J. C. Moore et al. (1991) for anomalous fault plane reflections along the Oregon accretionary prism. These authors suggest that the lateral velocity variations are caused by high, but variable, fluid pressures within the zones that allow the zones to become dilated. It is thus possible that the Nankai décollement is a zone of laterally variable fluid pressures (and therefore variable velocities and densities) caused by pulses of pore fluids from deep in the prism. The pulses of pore fluid moving along the décollement zone are less than a few tens of m in length both up dip and along strike, as indicated by the scale of the three-dimensional reflection waveform and amplitude variations.

SUMMARY AND CONCLUSIONS

The décollement in the Leg 131 area of the Nankai Trough is a 19-m-thick zone of intense shearing that is imaged seismically as a high-amplitude, reversed-polarity reflection. Synthetic seismic models show that the décollement signature can be modeled as a sharp decrease in velocity and density beneath the décollement. Velocities and densities within the décollement zone are not higher than those of the overlying strata; through much of the area décollement velocities/densities are lower, and in some places they may be significantly lower. The character of the décollement reflection varies laterally. Numerous thin layer models with complex overlying structures reveal that most of the variations in amplitude cannot be fully explained by either focusing/defocusing effects. The models confirm that changes in the décollement amplitude represent lateral changes in velocity and density within the thin décollement layer, which are in turn probably driven by fluid pressure variations beneath the décollement.

ACKNOWLEDGMENTS

Steffen Saustrop assisted in modeling the air-gun waveform. The final manuscript was clarified greatly by insightful reviews by Nathan Bangs and Don Reed. This work was supported by the National Science Foundation through grants OCE-8613707 to G.M. and OCE-8613774 and OCE-9000327 to T.S. and through a USSAC grant to G.M.

REFERENCES

Badley, M.E., 1985. *Practical seismic interpretation:* Boston (IHRDC Press).

Bangs, N.L.B., and Westbrook, G.K., 1991. Seismic modeling of the décollement zone at the base of the Barbados Ridge accretionary complex. *J. Geophys. Res.,* 96:3853–3866.

Gardner, G.H.F., Gardner, L.W., and Gregory, A.R., 1974. Formation velocity and density—the diagnostic basics of stratigraphic traps. *Geophysics,* 39:770–780.

Kallweit, R.S., and Wood, L.C., 1982. The limits of resolution of zero-phase wavelets. *Geophysics,* 47:1035–1046.

Karig, D.E., Moran, K., and Leg 131 Scientific Party, 1990. A dynamically sealed décollement: Nankai prism. *Eos,* 71:1626.

Knapp, R.W., 1990. Vertical resolution of thick beds, thin beds, and thin-bed cyclothems. *Geophysics,* 55:1184–1191.

Meckel, L.D., and Nath, A.K., 1977. Geologic considerations for stratigraphic modeling and interpretation. *AAPG Mem.,* 26:417–438.

Moore, G.F., Karig, D.E., Shipley, T.H., Taira, A., Stoffa, L., and Wood, W.T., 1991. Structural framework of the ODP Leg 131 area, Nankai Trough. *In* Taira, A., Hill, I., Firth, J.V., et al., *Proc. ODP, Init. Repts.,* 130: College Station, TX (Ocean Drilling Program), 15–20.

Moore, G.F., Shipley, T.H., Stoffa, P.L., Karig, D.E., Taira, A., Kuramoto, S., Tokuyama, H., and Suyehiro, K., 1990. Structure of the Nankai Trough accretionary zone from multichannel seismic reflection data. *J. Geophys. Res.,* 95:8753–8765.

Moore, J.C., Brown, K.M., Horath, F., Cochrane, G., MacKay, M., and Moore, G., 1991. Plumbing accretionary prisms: effects of permeability variations. *Philos. Trans. R. Soc. London A,* 335:275–288.

Moore, J.C., Mascle, A., Taylor, E., Andreieff, P., Alvarez, F., Barnes, R., Beck, C., Behrmann, J., Blanc, G., Brown, K., Clark, M., Dolan, J., Fisher, A., Gieskes, J., Hounslow, M., McLellan, P., Moran, K., Ogawa, Y., Sakai, T., Schoonmaker, J., Vrolijk, P., Wilkens, R., and Williams, C., 1988. Tectonics and hydrogeology of the northern Barbados Ridge: results from Ocean Drilling Program Leg 110. *Geol. Soc. Am. Bull.,* 100:1578–1593.

Neidell, N.S., and Poggiagliolmi, E., 1977. Stratigraphic modeling and interpretation—geophysical principals and techniques. *AAPG Mem.,* 26:389–416.

Stoffa, P.L., Wood, W.T., Shipley, T.H., Moore, G.F., Nishiyama, E., Botelho, M.A.D., Taira, A., Tokuyama, H., and Suyehiro, K., 1992. Deep water high resolution expanding spread and split-spread seismic profiles in the Nankai trough. *J. Geophys. Res., 97B:1687–1713.*

Sheriff, R.E., 1985. Aspects of seismic resolution. AAPG Mem., 39:1–10.

Shipboard Scientific Party, 1991. Site 808. *In* Taira, A., Hill, I., Firth, J.V., et al., *Proc. ODP, Init. Repts.,* 130: College Station, TX (Ocean Drilling Program), 71–269.

Widess, M.B., 1973. How thin is a thin bed? *Geophysics,* 38:1176–1180.

Date of initial receipt: 28 October 1991
Date of acceptance: 28 April 1992
Ms 131SR-111

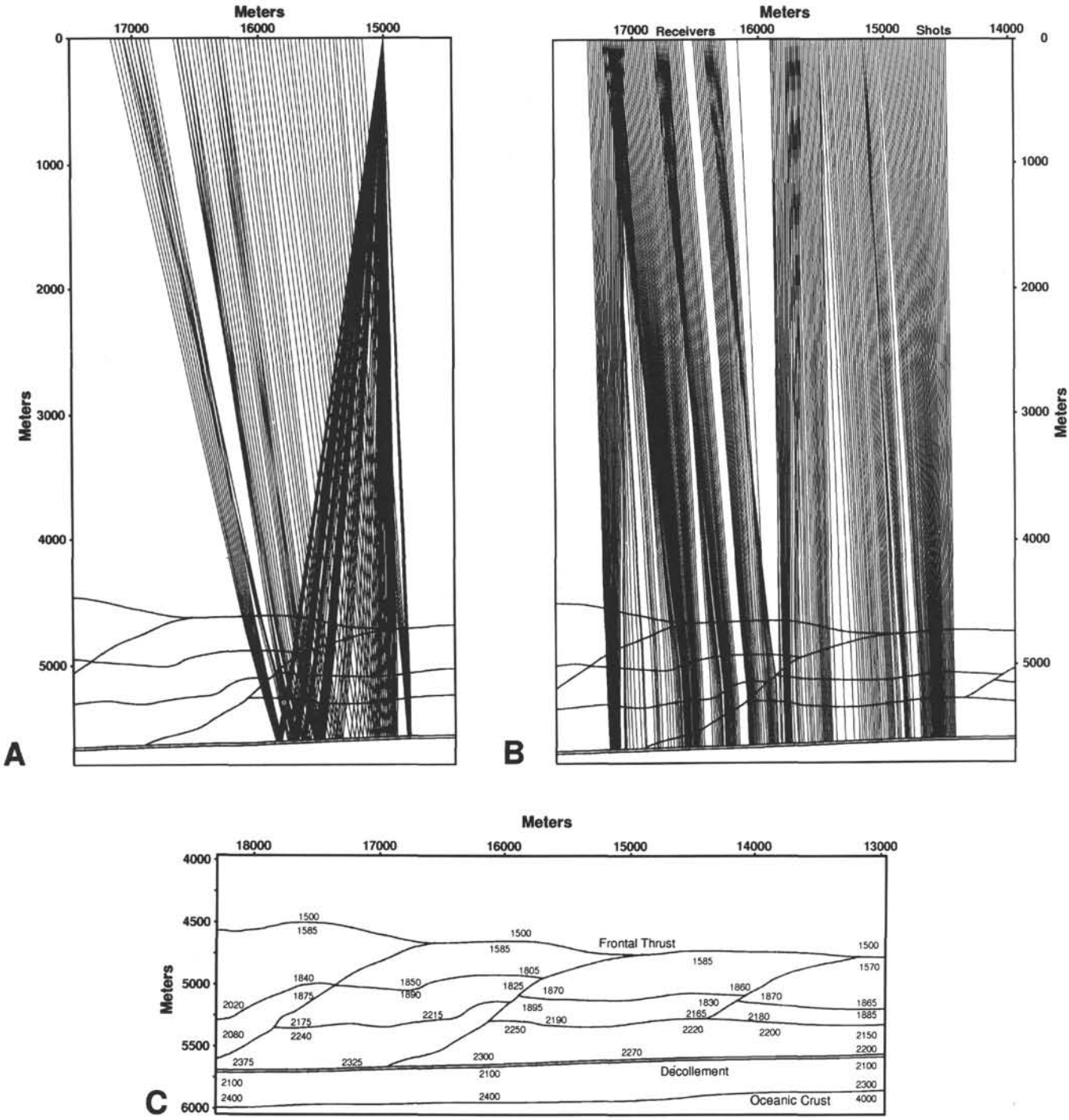

Figure 7. **A.** Ray-trace diagram for a single shot seaward of Site 808 and equally spaced receivers. Note focusing/defocusing effects. **B.** Zero-offset (stacked traces) ray-trace diagram that also shows focus/defocus effects. **C.** Velocity model used for ray tracing and two-dimensional wave equation modeling.

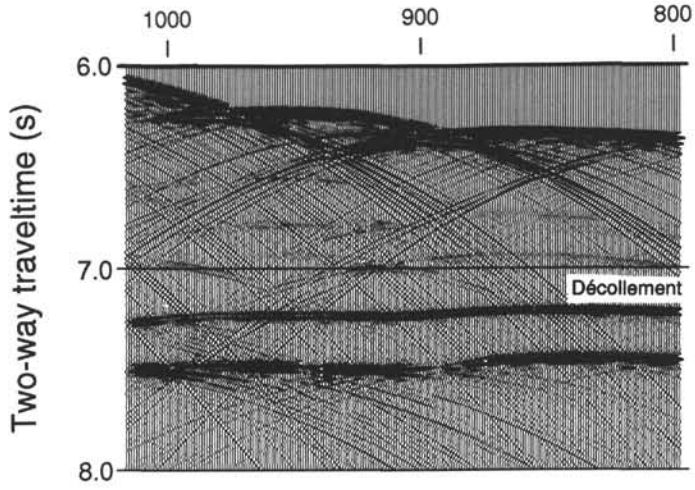

Figure 8. Synthetic seismic section produced by wave equation modeling using velocity model of Fig. 7C. Note lateral changes in amplitude of décollement reflection due to focusing/defocusing.

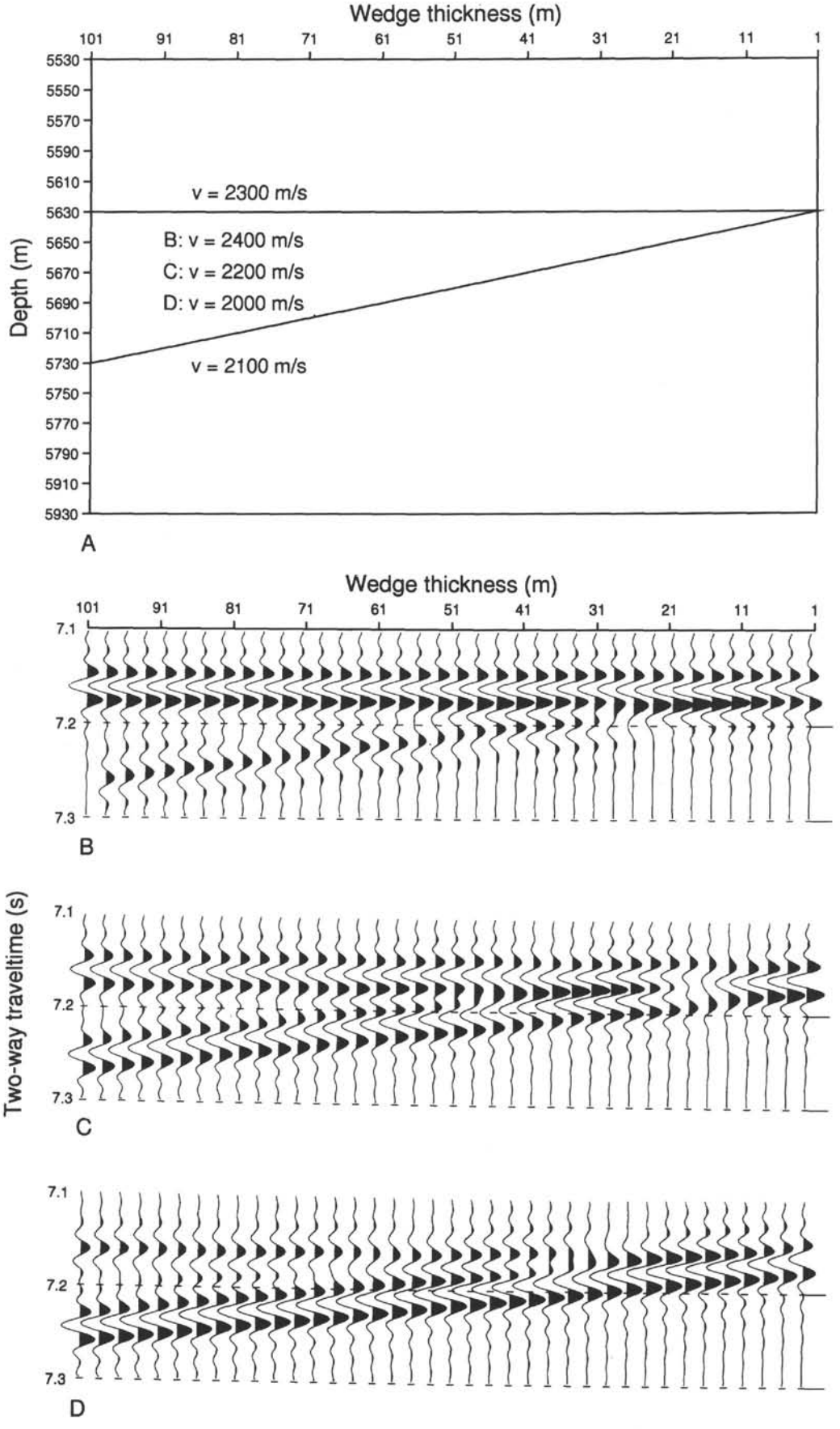

Figure 9. Synthetic seismic models of wedges that demonstrate the effects of layer thinning on amplitudes ("tuning effect"). **A.** Thinned wedge. **B.** Low-velocity zone. **C.** Intermediate-velocity zone. **D.** High-velocity zone.

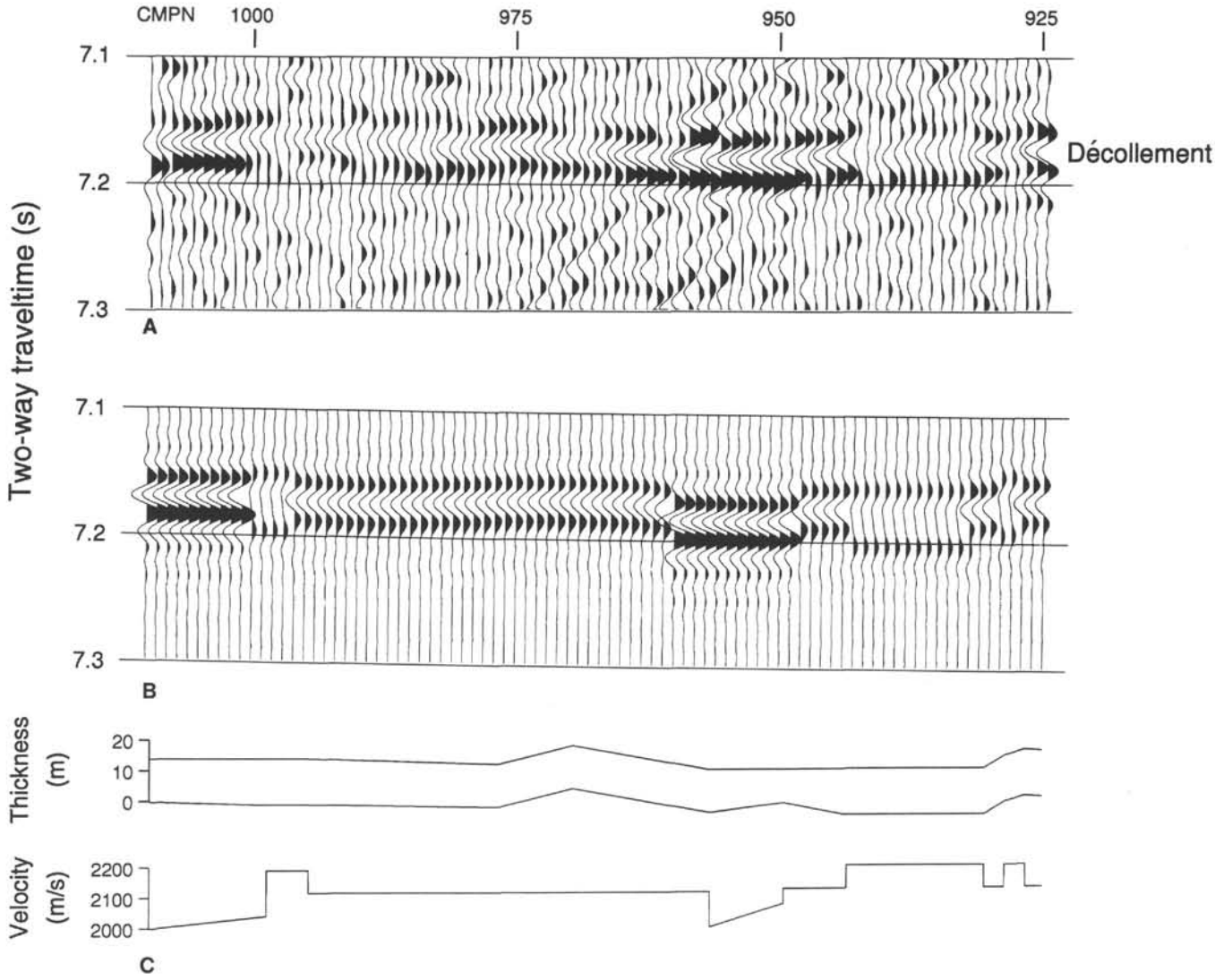

Figure 10. **A.** Detail of reprocessed stacked time section showing variations in amplitude and waveform laterally away from Site 808. **B.** Synthetic seismic section generated from thickness and velocity model below. **C.** Model with variation in thickness and velocity of décollement zone. Overlying velocity was constant at 2300 m/s and underlying velocity was constant at 2100 m/s. Within individual CMP gathers, the amplitude of the décollement reflection decreases with offset, indicating an increase in Poisson's ratio below the décollement. This is consistent with the interpretation that strata below the décollement have lower velocities due to their higher porosities.